08

# Effect of thermal annealing on properties Ga$_2$O$_3$/GaAs:Cr heterostructures

© *V.M. Kalygina, O.S. Kiseleva, V.V. Kopyev, B.O. Kushnarev, V.L. Oleinik, Y.S. Petrova, A.V. Tsymbalov*

Tomsk State University,
634050 Tomsk, Russia
e-mail: Kalygina@ngs.ru

Data on the sensitivity of Ga$_2$O$_3$/GaAs:Cr heterostructures are presented to long-wave and UV ($\lambda = 254$ nm) radiation. The samples were obtained by RF magnetron sputtering of a gallium oxide film on non-heated GaAs:Cr substrates. Gallium arsenide plates with a Ga$_2$O$_3$ film were divided into two parts: one half was not annealed, and the other was annealed in argon at 500°C for 30 min. Regardless of the presence or absence of heat treatment, the studied structures exhibit a photovoltaic effect and are able to operate in an autonomous mode. It is shown that a noticeable sensitivity to long-wave radiation appears in the samples only after thermal annealing of gallium oxide films. The response and recovery times of such UV radiation detectors do not exceed 1 second.

**Keywords:** dark current, photocurrent, UV radiation, Ga$_2$O$_3$/GaAs:Cr structures, autonomous operation mode.

## Introduction

Oxides are materials with high utilization capacity for creation of next generation electronic devices, including various types of deep-UV sensors and photodetectors whose advantage is in direct UV radiation conversion into electrical signal. Instruments that can be operated in self-contained mode are of particular interest. Such photodetectors have a simple design and, what is more important, are designed for direct integration with the metal−insulator−semiconductor (MIS) fabrication technology.

Among oxide compounds, large focus is made on sesquioxides (In$_2$O$_3$, Ga$_2$O$_3$, Al$_2$O$_3$) and their ternary alloys, because they have a wide band gap in a range from 3.7 eV for In$_2$O$_3$ to 8.9 eV for Al$_2$O$_3$ and are suitable for the development of many devices such as power diodes and transistors, gas detectors and UV photodetectors. Most research and development have been still aimed at the investigation of Ga$_2$O$_3$, because this compound has thermodynamically stable polymorphous phases and can be easily prepared in the form of single crystals [1], thin epitaxial layers [2] and nanostructure [3].

The properties of gallium oxide films and characteristics of the metal/Ga$_2$O$_3$ interface and semiconductor/Ga$_2$O$_3$ heterojunction depend on the production method, thickness of the applied layers [4], in-process gas mixture pressure [5,6] as well as on post-treatment procedures [7,8]. On the other hand, processes at these boundaries define electrical and optical specifications of structures based on thin gallium oxide layers. Heterostructures based on Ga$_2$O$_3$/GaAs are of practical interest that is explained by low density of states at the interface that may achieve $D_{it} = 1 \cdot 10^{10}-1 \cdot 10^{11}$ cm$^{-2}$ eV$^{-1}$ [9,10]. Besides, high electron mobility in gallium arsenide allows fast-response instruments to be designed [11,12].

Currently, the structures made on the basis of Ga$_2$O$_3$/GaAs are understrudied, therefore the aim of this study is to investigate the effect of heat annealing on the properties of these heterostructures.

## 1. Experiment procedure

Electrical and photovoltaic properties of Ga$_2$O$_3$/GaAs:Cr structures have been investigated herein. Chromium-doped *n*-GaAs layers with orientation (100), resistivity of $10^9$ Ω·cm were used (Figure 1).

120−150 nm gallium oxide films was produced by the HF magnetron sputtering of Ga$_2$O$_3$ (3N) target on the heated GaAs:Cr substrates using AUTO-500 unit (Edwards) in Ar/O$_2$ gas mixture. Oxygen concentration in the mixture was maintained at $56.1 \pm 0.5$ vol.%. The target-to-substrate distance was 70 mm. Chamber pressure during sputtering was maintained at 0.7 Pa. After oxide application, the substrate with Ga$_2$O$_3$ film was divided into two parts: one part of samples was not subjected to heat treatment, and the other half was annealed in argon at 500°C during 30 min.
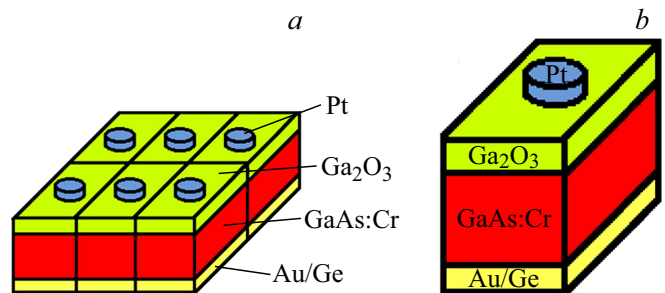


**Figure 1.** Ga$_2$O$_3$/GaAs:Cr HF structures: GaAs substrate with applied Ga$_2$O$_3$ layers and metal contacts (*a*); view of individual sample (*b*).
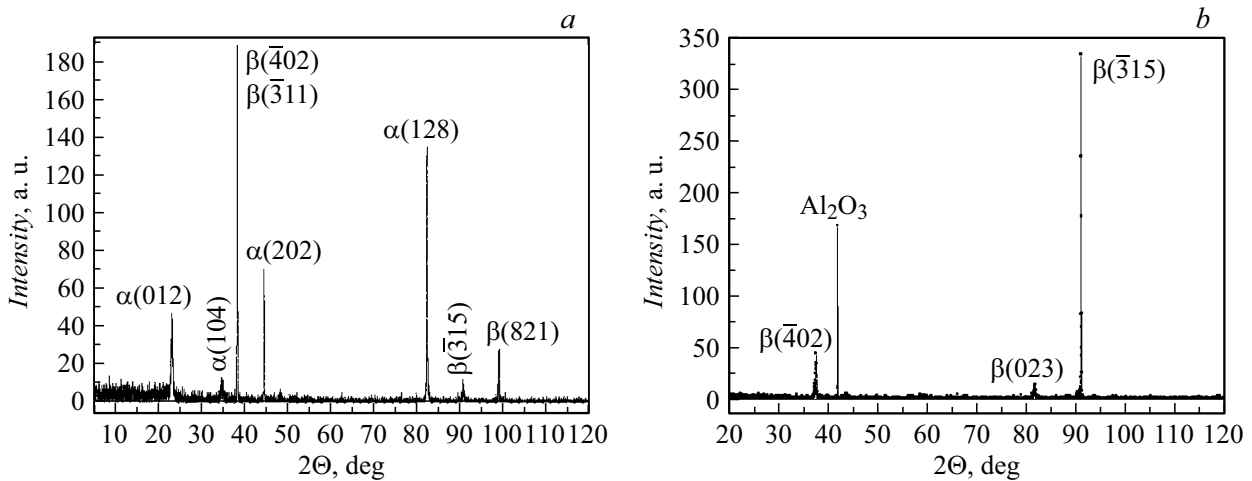
**Figure 2.** X-ray diffraction analysis spectra of gallium oxide films: *a* — without annealing; *b* — after annealing in Ar at 900°C.

gallium oxide film structure and phase composition was defined by the X-ray diffraction analysis (XDA) method using Lab-X XRD 6000 Shimadzu X-Ray diffractometer.

For electrical measurements, contacts were applied to Ga$_2$O$_3$ surface and to the rear of the semiconductor substrate: the electrode to the semiconductor was made in the form of solid metal film (Au/Ge), and the electrode to gallium oxide was applied by Pt sputtering through masks (Figure 1). The area of the contact to Ga$_2$O$_3$ was equal to $1.04 \cdot 10^{-2}$ cm$^2$.

Dark current-voltage curves (CVC) and CVC under ultraviolet radiation exposure were examined at room temperature using Keithley 2611B and Keithley 2636A source meters. Krypton-fluorine lamp VL-6.C with a 254 nm filter was used as the UV source. The distance between the lamp and sample was equal to 1 cm, and the radiation intensity was 0.78 mW/cm$^2$. The effect of longwave radiation was investigated using the white LED light with the total power of $3 \cdot 10^{-3}$ W, or $\lambda = 532$ nm laser.

## 2. Experimental data and discussion

### 2.1. X-ray diffraction analysis data

Figure 2 shows the X-ray diffraction analysis data for gallium oxide films without annealing (Figure 2, *a*) and after annealing in inert atmosphere at 900°C (Figure 2, *b*). The applied oxide film without heat treatment may be assumed as an amorphous matrix with integrated individual $\alpha$- and $\beta$-phase Ga$_2$O$_3$ grains with various crystal-lattice orientation (Figure 2, *a*). After annealing in argon during 30 min, the film becomes fully crystalline and contains only $\beta$-phase grains (Figure 2, *b*).

Reflection gain in XDA spectra of gallium oxide films with increasing annealing temperature was observed by X. Zhang et al [13].

### 2.2. Electrical and photovoltaic characteristics of samples without annealing

Dark CVC of Ga$_2$O$_3$/GaAs:Cr structures are asymmetric with respect to voltage polarity (Figure 3). Rectification factor at $U = \pm 1$ V is equal to 4.7. Direct CVC branches are observed at negative gate potentials. Reverse dark current density ($I_D$) at $U = +4.5$ V is equal to $4 \cdot 10^{-9}$ A/cm$^2$. Thus, GaAs:Cr in the studied structures demonstrates the properties of *p*-type semiconductor.

When exposed to $\lambda = 254$ nm UV radiation, growth of currents is observed irrespective of the gate potential sign (Figure 4, curve $I_{L1}$).

When voltage is further applied to the structure during continuous UV radiation exposure, photocurrents increase and then are stabilized (Figure 4, curves $I_{L2} - I_{L4}$). Higher photocurrents were obtained at positive gate potentials (Figure 5).
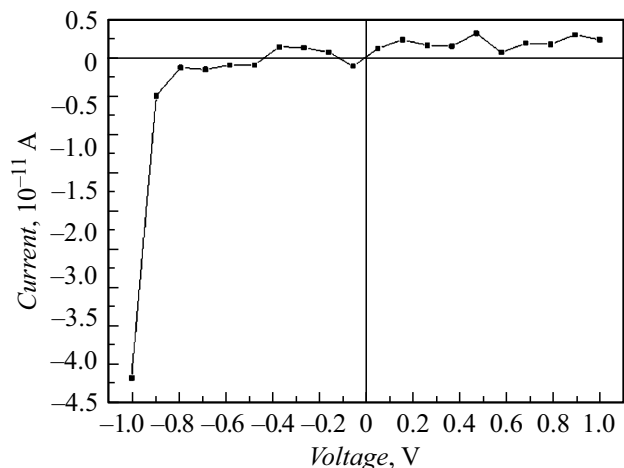


**Figure 3.** Dark CVC of Ga$_2$O$_3$/GaAs:Cr structure without annealing.

Data analysis in Figures 4 and 5 shows that, when exposed to shortwave radiation, currents $I_L$ are higher that the dark current of samples by an order of magnitude and more both at negative and positive gate potentials. This allows to use such structures as UV radiation detectors. The presence of response at $U = 0$ V suggests that such photodiodes are capable of operating in offline mode. The Table shows no-load voltages $U_{idl.}$ and short-circuit currents $I_{sh.cir.}$ for several samples.
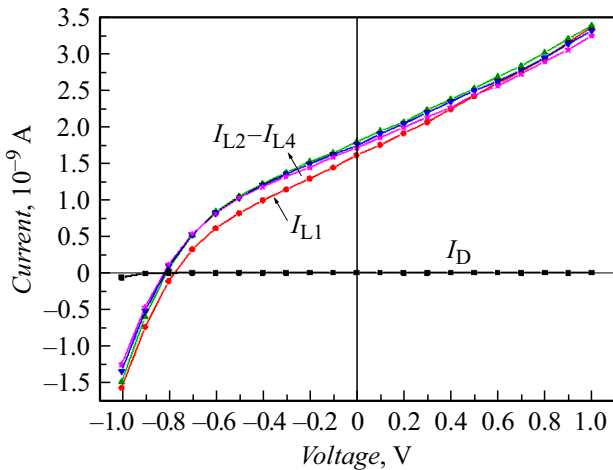
The contrast defined by the light-to-dark current ratio ($I_L/I_D$) depends on the sample voltage (Figure 6).

Figure 6 shows that it is more feasible to use $Ga_2O_3/GaAs:Cr$ structures as UV radiation detectors at positive potentials at contacts to the oxide film.
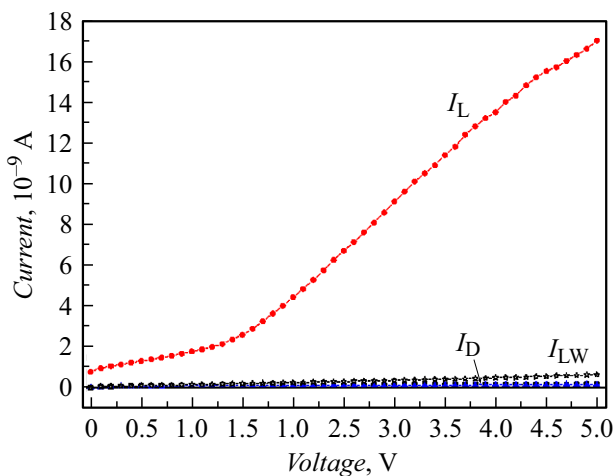
The samples without annealing are low sensitive to high-intensity white light and, therefore, they may be treated as solar-blind. Figure 5 shows dark currents ($I_D$) measured

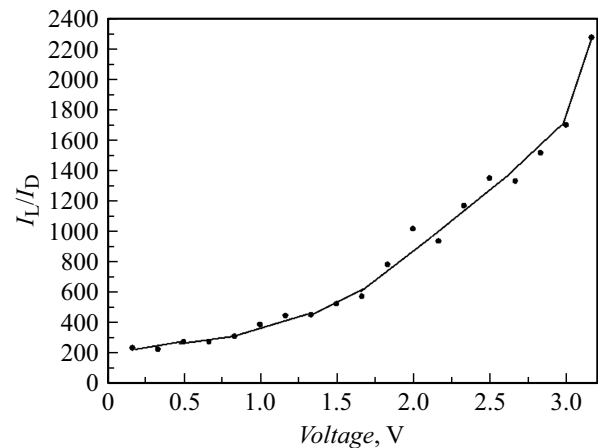$U_{idl.}$ and $I_{sh.cir.}$ values for $Ga_2O_3/GaAs:Cr$ structures exposed to $\lambda = 254$ nm UV radiation

| Sample № | $U_{idl.}$, V | $I_{sh.cir.}$, A |
|---|---|---|
| 1 | 0.82 | $1.72 \cdot 10^{-9}$ |
| 2 | 0.80 | $8.0 \cdot 10^{-9}$ |
| 3 | 0.95 | $1.3 \cdot 10^{-8}$ |
| 4 | 0.82 | $7.4 \cdot 10^{-9}$ |
| 5 | 0.97 | $9.3 \cdot 10^{-10}$ |



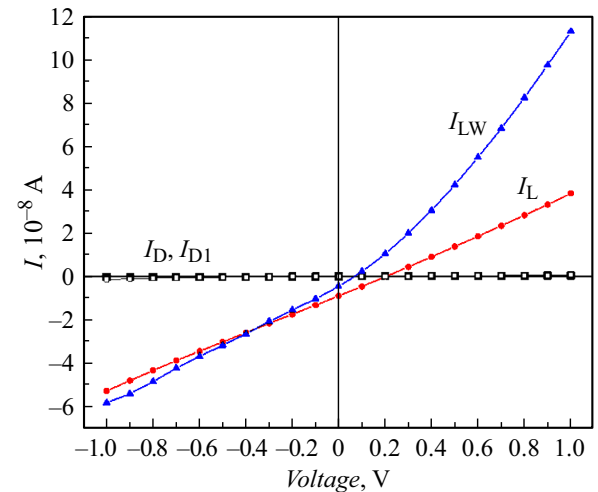**Figure 6.** Dependence of $I_L/I_D$ on voltage (positive potentials on Pt electrode).



**Figure 4.** CVC of $Ga_2O_3/GaAs:Cr$ sample: dark ($I_D$) at positive and negative gate potentials and when $\lambda = 254$ nm UV radiation is applied ($I_{L1} - I_{L4}$).



**Figure 7.** CVC of $Ga_2O_3/GaAs:Cr$ structures with gallium oxide film after annealing at 500°C: dark current ($I_D$); current during $\lambda = 254$ nm radiation exposure ($I_L$); dark current after removal of UV ($I_{D1}$); current during white light exposure ($I_{LW}$).



**Figure 5.** CVC of $Ga_2O_3/GaAs:Cr$ sample at positive gate potentials: dark (ID), with $\lambda = 254$ nm ($I_L$) UV radiation exposure, with exposure to three white LEDs ($I_{LW}$).
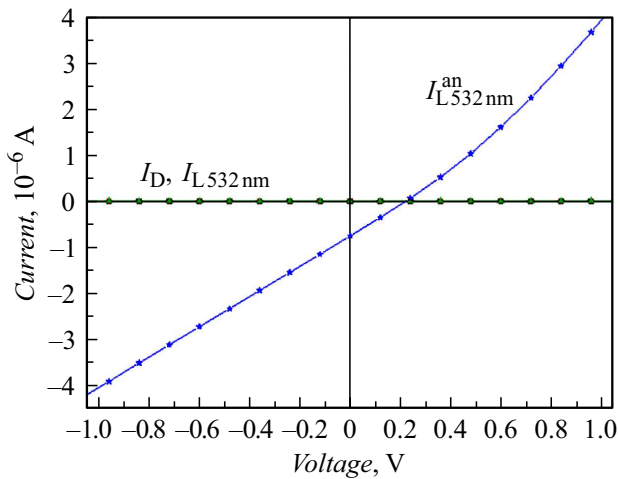
at positive gate potentials, photocurrent during exposure to $\lambda = 254$ nm ($I_L$) radiation and when the sample is exposed to $3 \cdot 10^{-3}$ W white diode light ($I_{LW}$) from the oxide film side. At $U = 5$ V, photocurrent $I_L = 1.7 \cdot 10^8$ A, while $I_{LW} = 6.3 \cdot 10^{-10}$ A.
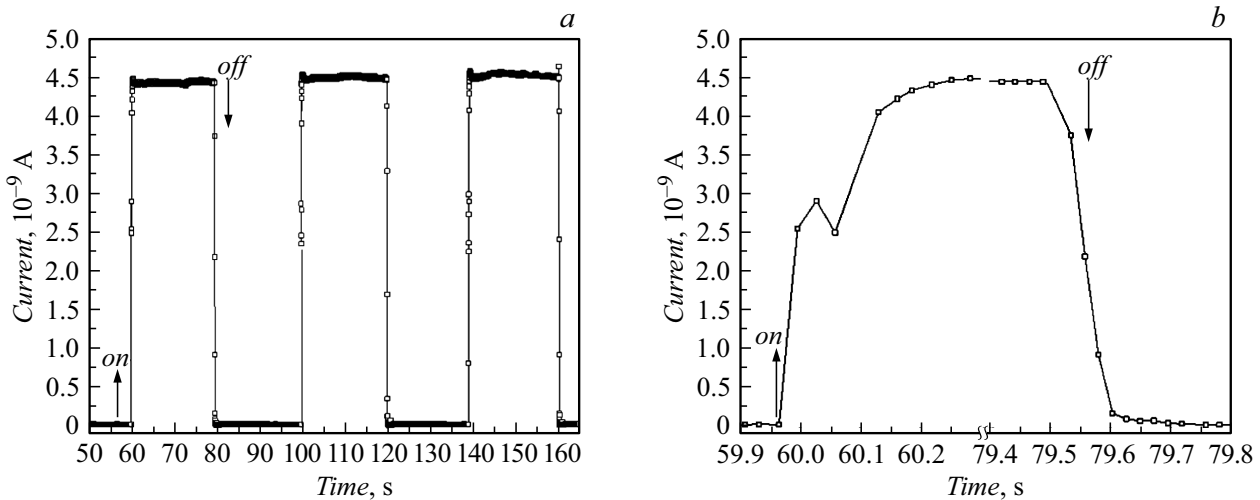
**Figure 8.** Current-voltage dependences of Ga$_2$O$_3$/GaAs: Crstructures with gallium oxide film and after annealing at 500°C: dark current without annealing ($I_D$); current during $\lambda = 532$ nm white light exposure of the sample without annealing ($I_{L\,532\,nm}$); sample current after annealing during $\lambda = 532$ nm ($I_{L\,532\,nm}^{an}$) radiation exposure.

However, if GaAs:Cr substrates with the sputtered gallium oxide layer are annealed in argon at 500°C during 30 min, then Ga$_2$O$_3$/GaAs:Cr structures become sensitive to longwave radiation.

## 2.3. Electrical and photovoltaic characteristics of samples after annealing

Figure 7 shows dark CVC($I_D$, $I_{D1}$) and CVC when samples are exposed to$\lambda = 254$ nm ($I_L$) radiation and $3 \cdot 10^{-3}$ W ($I_{LW}$) white light from the oxide film side.

Curve $I_{D1}$ corresponds to the dark current measured immediately after removal of UV radiation.

The structures respond to $\lambda = 532$ nm laser exposure with a higher power in a similar way. Figure 8 shows the effect of $\lambda = 532$ nm radiation on CVC of the samples without annealing ($I_{L\,532\,nm}$) and after annealing in argon during 30 min at500°C ($I_{L\,532\,nm}^{an}$).
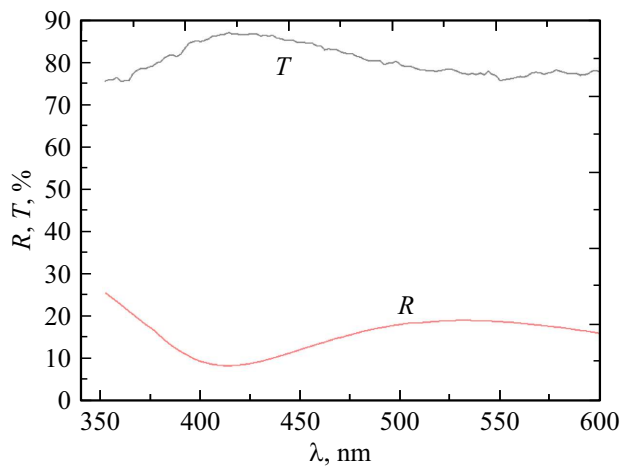
Similar annealing effect on the sensitivity of Ga$_2$O$_3$/semiconductor structures to visible radiation was previously observed by us for Ga$_2$O$_3$/$n$-GaAs samples with anodic gallium oxide film [7].

Annealing at high temperature affects not only optical properties of Ga$_2$O$_3$/GaAs:Cr structures, but also results in the change of the type of conductivity of GaAs:Cr. After annealing, high-resistance GaAs:Cr substrate in Ga$_2$O$_3$/GaAs:Cr heterostructures shows the properties of $n$-type semiconductor: independently of the incident radiation wavelength, no-load voltage is observed at positive gate potentials (Figure 7, 8).

Photodetectors based on Ga$_2$O$_3$/GaAs:Cr structures contain virtually no residual currents that are often observed in various types of devices capable of detecting UV radiation [14–16]. Time parameters of the samples studied in herein are characterized by low response time ($t_r$) and recovery time ($t_d$). Figure 9 shows current variation pulses at $U = 3$ V on the sample with enabled and disabled $\lambda = 254$ nm radiation.

photocurrent rise time ($t_r$) and fall time ($t_d$) do not exceed 1 s that is confirmed by data in Figure 9, $b$, and therefore Ga$_2$O$_3$/GaAs:Cr structures may be considered as being fast response. Higher sensitivity of Ga$_2$O$_3$/GaAs:Cr structures to longwave radiation after annealing is explained by increased transmittance of the oxide film (about 80%) (Figure 10).

On the other hand, increasing transmittance $T$ of gallium oxide films after annealing may be due to Ga$_2$O$_3$ transition



**Figure 9.** Time dependences of current variation in Ga$_2$O$_3$/GaAs:Cr structure with enabled and disabled $\lambda = 254$ nm radiation: $a$ — current-time profile for three pulses; $b$ — zoomed-in start and end of the first pulse.

**Figure 10.** Transmittance spectrum ($T$) and reflectance spectrum ($R$) of $Ga_2O_3$ film after annealing.

from partially amorphous to polycrystalline state.

## Conclusion

The study has investigated $Ga_2O_3$/GaAs:Cr structures that use high-resistance gallium arsenide layers made by Cr diffusion into *n*-GaAs as a substrate. The samples show sensitivity to $\lambda = 254$ nm UV radiation and are low sensitive to longwave radiation provided that the gallium oxide films deposited on the GaAs:Cr surface are not annealed at high temperatures. Response and recovery times of such UV detectors do not exceed 1 s.

### Funding

### Conflict of interest

The authors declare that they have no conflict of interest.

## References

[1] W. Mi, J. Ma, Z. Li, C. Luan, H. Xiao. J. Mater. Sci.: Mater. Electron, **26**, 7889 (2015). DOI: 10.1007/s10854-015-3440-2

[2] Y. Zhang, F. Alema, A. Mauze, O.S. Koksaldi, R. Miller, A. Osinsky, J.S. Speck, APL Mater., **7**, 022506 (2019). https://doi.org/10.1063/1.5058059

[3] T. Uchida, R. Jinno, S. Takemoto, K. Kaneko, S. Fujita, Jpn. J. Appl. Phys., **57** (4), 040314 (2018). DOI: 10.7567/JJAP.57.040314

[4] X. Wang, Z. Chen, D. Guo, X. Zhang, Z. Wu, P. Li, W. Tang. Opt. Mater. Express, **8** (9), 2918 (2018). https://doi.org/10.1364/OME.8.002918

[5] Z. Li, Z. An, Y. Xu, Y. Cheng, Y. Cheng, D. Chen, Q. Feng, S. Xu, J. Zhang, C. Zhang, Y. Hao. J. Mater. Sci., **54**, 10335 (2019).

[6] M.-Q. Lia, N. Yanga, G.-G. Wanga, H.-Y. Zhanga, J.-C.Hana. Appl. Surf. Sci., **471**, 694 (2019). https://doi.org/10.1016/j.apsusc.2018.12.045

[7] V.M. Kalygina, V.V. Vishnikina, Yu.S. Petrova, I.A. Prudaev, T.M. Yaskevich. FTP, **49** (3), 357 (2015) (in Russian).

[8] J. Yua, J. Louc, Z. Wang, S. Jic, J.Chend, M. Yub, B. Peng, Y. Hu, L. Yuan, Y. Zhang, R. Jia. J. Alloys Compd., **872**, 159508 (2021).

[9] M. Hong, J.P. Mannaerts, J.E. Bower, J. Kwo, M. Passlack, W.-Y. Hwang, L.W. Tu. J. Cryst. Growth, **175**, 422 (1997).

[10] M. Holland, C.R. Stanley, W. Reid, R.J.W. Hill, D.A.J. Moran, I. Thayne, G.W. Paterson, A.R. Long. J. Vac. Sci. Technol. B, **25**, 1706 (2007). https://doi.org/10.1116/1.2778690

[11] J. Hwang, C.C. Chang, M.F. Chen, C.C. Chen, K. Lin, F.C. Tang, M. Hong, J. Kwo. J. Appl. Phys., **94** (1), 348 (2003).

[12] P.D. Ye, G.D. Wilk, B. Yang, J. Kwo, G. Chu, S. Nakahara, J.P. Mannaerts, M. Hong, K.K. Ng, J.D. Bu. Appl. Phys. Lett., **83** (1), 180 (2003).

[13] X. Zhang, D. Jiang, M. Zhao, H. Zhang, M. Li, M. Xing, J. Han, A.E. Romanov. J. Phys.: Conf. Series, **1965**, 012066 (2021). DOI: 10.1088/1742-6596/1965/1/012066.

[14] B.R. Tak, M.-M. Yang, M. Alexe, R. Singh. Cryst., **11** (9), 1046 (2021). https://doi.org/10.3390/cryst11091046

[15] L. Huang, Q. Feng, G. Han, F. Li, X. Li, L.Fang, X. Xing, J. Zhang, Y. Hao. IEEE Photon. J., **9** (4), 6803708 (2017).

[16] Y. Qin, S. Long, H. Dong, Q. He, G. Jian, Y. Zhang, X. Hou, P. Tan, Z. Zhang, H. Lv, Q. Liu, M. Liu. Chin. Phys. B, **28** (1), 018501 (2019). DOI: 10.1088/1674-1056/28/1/018501

*Translated by Ego Translating*